ISSN: 2692-5397
DOI: 10.33552/MCMS.2024.05.000620
Modern Concepts in Material Science
Iris Publishers
Research Article
Copyright © All rights are reserved by Letterio Mavilia

XRD, FTIR and RAMAN Characterizations of Metakaolin Geopolymers

Giuseppe Mavilia[1], Maria Teresa Caccamo[2], Letterio Mavilia[3]* and Salvatore Magazù[2]

[1]*Istituto per i Processi Chimico-Fisici, Consiglio Nazionale delle Ricerche, V. le F.S. d' Alcontres 37, 98158 Messina, Italy*

[2]*Dipartimento di Scienze Matematiche e Informatiche, Scienze Fisiche e Scienze della Terra, Università di Messina, Viale Ferdinando Stagno D'Alcontres n 31, S. Agata, 98166 Messina, Italy*

[3]*Dipartimento Patrimonio, Architettura, Urbanistica (PAU); Università Mediterranea di Reggio Calabria, Via dell'Università 25 - 89124 Reggio Calabria, Italy*

***Corresponding author:** Letterio Mavilia, Dipartimento Patrimonio, Architettura, Urbanistica (PAU); Università Mediterranea di Reggio Calabria, Via dell'Università 25 - 89124 Reggio Calabria, Italy.

Received Date: January 11, 2024

Published Date: January 24, 2024

Abstract

Nowadays, the production of materials with reduced energy consumption and environmental impact is of considerable interest. In this sense, geopolymers can be considered as important alternatives to Portland cement, as they allow a significant reduction in CO2 emissions and have high mechanical properties and thermal and chemical resistance. In this experimental research, it was decided to prepare geopolymers from metakaolin: this precursor has, in fact, considerable chemical reactivity and allows the production of geopolymers with reduced setting times and with excellent mechanical properties. The characterization of precursors (kaolin and metakaolin) and metakaolin geopolymers was performed using X-ray diffractometry (XRD), Fourier transform infrared spectroscopy (FTIR) and Raman spectroscopy. These techniques have highlighted both the complete transformation by calcination of crystalline kaolin into amorphous metakaolin and the formation of a metakaolin-based geopolymeric paste.

Keywords: Metakaolin; Geopolymers; FTIR spectroscopy; Calcination treatment; Raman spectroscopy

Introduction

Geopolymers are a class of inorganic polymeric materials obtained by a chemical reaction between a reactive aluminosilicate raw material (metakaolin, volcanic ash, fly ash, blast furnace slag, kaolin, zeolite) and an activating alkaline solution. The geopolymerization process takes place at room temperature or in any case at temperatures below 300°C also according to the characteristics of the desired product. In the case of the use of aluminosilicate powders, they should have a silica and alumina content of more than eighty percent by weight (SiO_2+Al_2O_3>80%wt.) in order to be considered as suitable raw materials to make geopolymers for structural applications. As regards their classification, geopolymers can be considered a subset of both alkaline-activated cements and inorganic polymers, characterized by a reduced calcium content and a high alumina content [1]. Two types of reagents must be selected to prepare a geopolymer (Figure 1): the precursor based on aluminosilicate powders (metakaolin, fly ash, blast furnace slag and volcanic ash) and the activating alkaline solutions (alkali metals, commonly NaOH and sodium silicate, generally Na_2SiO_3). As regards the choice of the precursor [2], metakaolin is the most used raw materials for the production of geopolymers, because they exhibit a higher reactivity than the other raw materials (metakaolin>zeolite>blast furnace slag>fly ash>volcanic ash). In fact, a high reactivity of the aluminosilicate raw materials promotes the alkaline hydrolysis of the same powders in the activating alkaline solution. Furthermore, the advantages

This work is licensed under Creative Commons Attribution 4.0 License

linked to the use of metakaolin as a precursor for the preparation of geopolymers are linked to the reversibility of the process, to the remarkable reactivity and chemical purity of the metakaolin, which favors the formation of the geopolymeric matrix: in fact, thanks to this precursor it is possible to obtain geopolymers characterized by important mechanical properties and with reduced setting times, which are applicable in the field of restoration of cultural heritage [3, 4]. Furthermore, other fillers such as carbon nanotubes (CNTs), polypropylene fibers (PP), glass fibers or stainless steel particles can also be added to the geopolymeric paste to increase the flexural strength of the geopolymer (Figure 2). Once the raw materials are mixed, the dissolution and consolidation reactions of the geopolymeric mixture take place at temperatures higher than the ambient temperature and in general between 40 and 200°C.

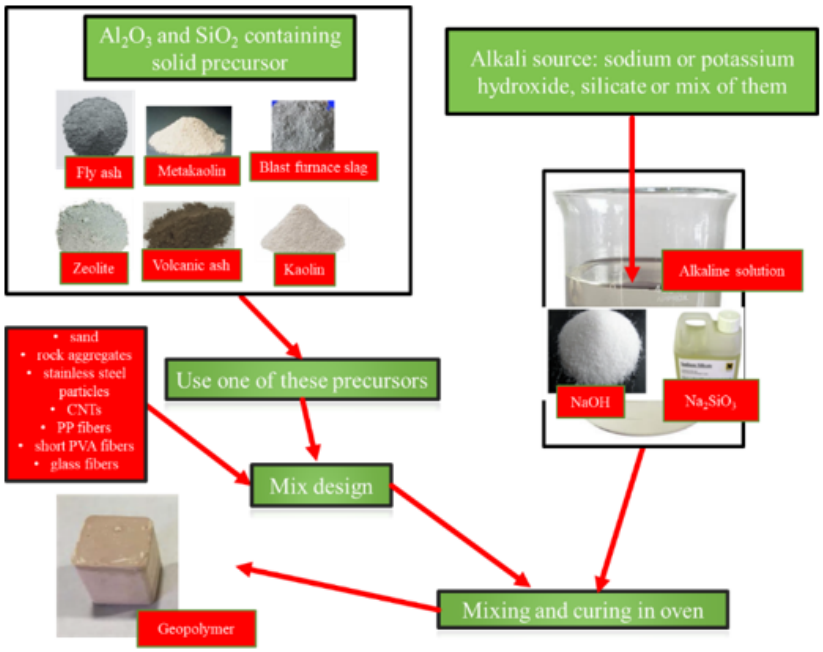

Figure 1: Scheme of preparation of geopolymers.

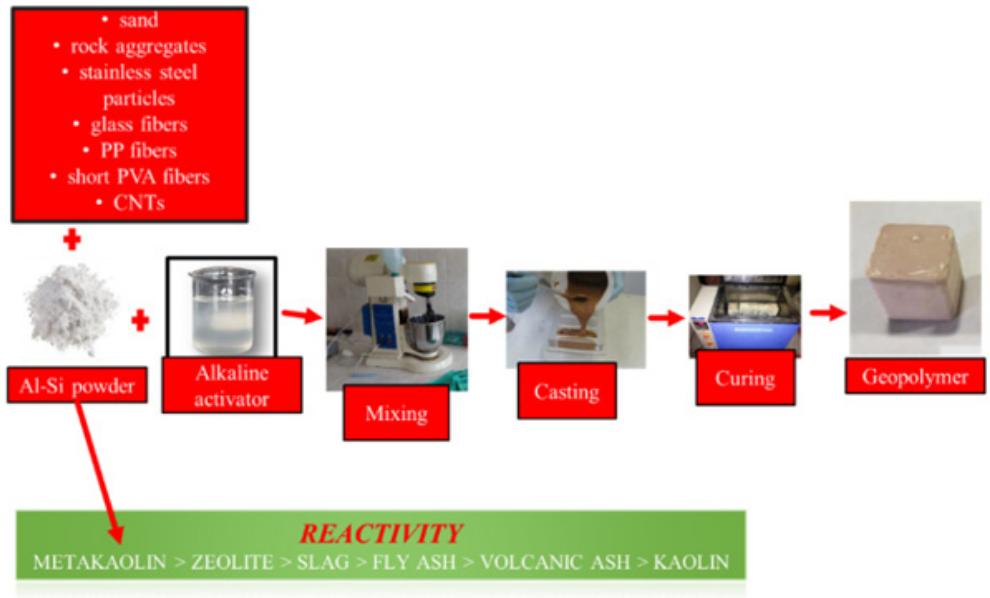

Figure 2: Easy and inexpensive geopolymers preparation process.

Geopolymerization is considered as the analogue of the synthesis of zeolites: the chemistry involved is similar, although the final products are different in composition and structure. In fact, zeolites possess a defined stoichiometric composition and crystalline structure, while geopolymers are mixtures of amorphous to semi-crystalline structures [5,6]. The process of geopolymer formation involves the dissolution of the aluminosilicate-based precursors in an activating alkaline solution (alkaline hydrolysis): after carrying this hydrolysis phase, there is initially the condensation phase with the consequent formation of a gel and, then, the polycondensation polymerization with the elimination of a water molecules and, finally, hardening of the paste [7-12]. Figure 3 illustrates the overall polymerization process in alkali-activated geopolymers.

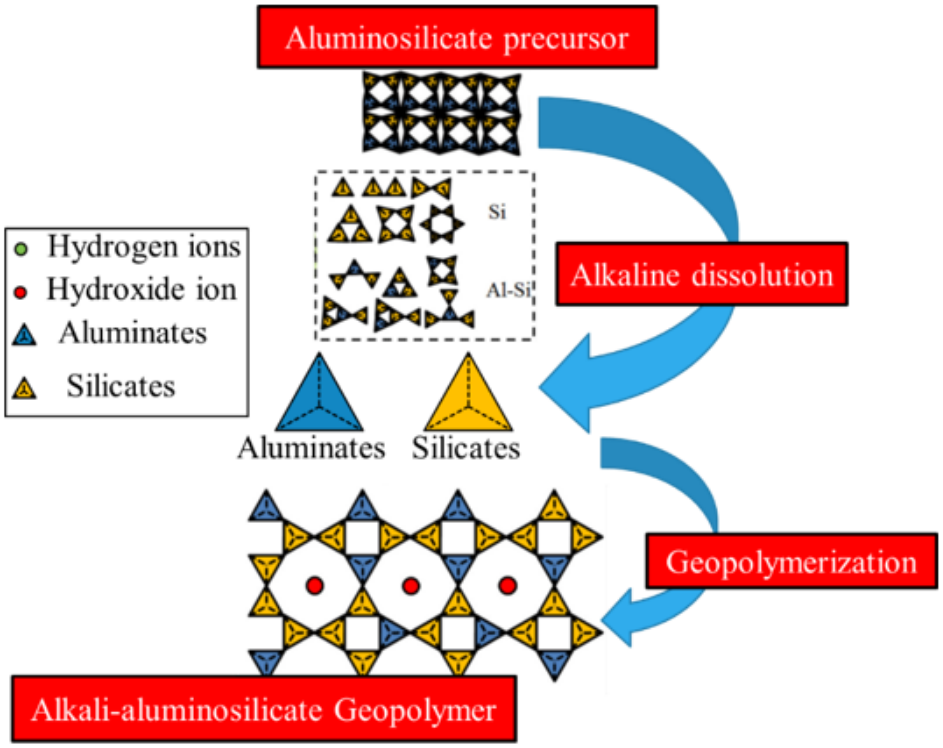

Figure 3: Polymerization process in alkali-activated geopolymers [7].

At the end of this process, an amorphous structure is obtained with a short-range order: it is a three-dimensional structure at the base of which there are tetrahedra of $(SiO_4)^{4-}$ and $(AlO_4)^{5-}$, connected by means of oxygen atoms [13]. The main properties of geopolymers are: rapid hardening, high resistance to compression and abrasion, resistance to flame over 1000°C without emission of toxic gases, high chemical resistance to acids and saline solutions, minimum dimensional shrinkage and low thermal conductivity. Furthermore, if used as an alternative to Portland cement, they reduce CO_2 emissions and have a lower cost of 10÷30% less than Portland cement when the source of alumino-silicate is constituted by fly ash. In addition, a comparison of both the physical-mechanical properties and those relating to the environmental impact of geopolymers with respect to Portland cement can be reported in the following Table 1.

Table 1: Properties and environmental impact of geopolymers compared to Portland cement [15].

Properties		Portland cement	Portland cement	Remarks
Environmental impact	CO_2 emission	800–900 kg/ton	150–200 kg/ton	CO2 emission in GP is during production of alkali hydroxide and silicate from carbonates
	Embodied Energy Water requirement	4000– 4400 MJ/ton ~600 L/ton	2200–2400 MJ/ton ~450 L/ton	As it mostly uses waste and by-products with no embodied energy GP do not need curing with water unlike Portland cement

Physic-mechanical properties	Setting time	30–300 min	10–60 min	Usually set faster than Portland cement, but depends on raw material reactivity and alkali concentration
	Compressive Strength Durability	33–53 MPa after 28 days Moderate	30–120 MPa after 27 days More durable than Portland cement	Strength can be tailored by optimizing raw material reactivity and alkali concentration GP systems are alumino-silicate based system which are resistant to acid attack

From Table 1, it can be seen that the geopolymers have lower setting times than Portland cement, therefore the hardening phase occurs more quickly in the former than Portland cement and, moreover, this step does not require the presence of water unlike Portland cement. Furthermore, geopolymers have greater compressive strength and greater durability than Portland cement, with a reduction of the CO_2 emissions produced, therefore with a reduced environmental impact. Furthermore, compared to Portland cement, the preparation process of a geopolymer does not determine the emission of NO_x, SO_x and CO, in addition to determining a reduced amount of CO_2 [14,15]. A very important parameter to evaluate for these materials is the Si/Al ratio, through which it is possible to evaluate the spatial development of the geopolymer. In fact, for values of the Si/Al ratio between 1 and 3, the geopolymer has a three-dimensional lattice: all geopolymers potentially usable in substitution of cement for applications in construction or as inert matrices to store hazardous waste have values of the Si/Al ratio all within this range. For values of this Si/Al ratio greater than 3, the geopolymer mainly presents a two-dimensional lattice: in the event that Si/Al values equal to 35 are reached, the geopolymers produced are mainly used as adhesives. Fiber-reinforced geopolymers are used for high temperature applications, such as foundry molds, thermal insulation panels and walls, flame retardant materials for use in automotive and aeronautics. For these applications, geopolymers prepared mainly from raw materials such as metakaolin are required [16]. In this experimental work, geopolymers were prepared from metakaolin: this precursor was effectively calcined at T=750°C for 3h and, then, it is mixed with an 8M NaOH solution with sodium trisilicate powders in order to effect the geopolymerization process at T=80°C. The characterization of both the starting material (kaolin) and the precursors (metakaolin) and of the metakaolin hardened geopolymer pastes was carried out using X-ray diffractometry (XRD), Fourier Transform Infrared Spectroscopy (FTIR) and Raman Spectroscopy. These techniques highlighted both the complete conversion of crystalline kaolin into amorphous metakaolin and the formation of the typical amorphous structure of the geopolymers.

Materials and Methods

Preparation of metakaolin based geopolymer

The reagents used for the preparation of the geopolymers are: kaolin (Riedel-de Haen) in the form of fine powder, sodium hydroxide pellets (Sigma Aldrich) and sodium trisilicate powder $Na_2Si_3O_7$ (Fluka). The calcination of the kaolin was carried out by heat treatment at a temperature of 750°C for a time of 3 hours: following this calcination, the kaolin (K) was converted into metakaolin (MK). Subsequently, the preparation of the activating alkaline solution was carried out: to do this, sodium trisilicate powders were dissolved in an 8M solution of sodium hydroxide in an amount equal to 6 parts by weight of solid and 8 parts by volume of liquid. The geopolymeric mixture was prepared by adding and slowly mixing in a moplen mold the solid and the liquid in the ratio of 8 parts by weight of metakaolin (MK) and 12 parts by weight of the activating solution prepared as described above. The geopolymeric mixture, covered with a non-hermetic lid, was cured in a climatic chamber (Angelantoni model Challenge 160) at a temperature of 80°C and relative humidity values of 70% for about 1 hour: later, this consolidation phase of the metakaolin geopolymer in the climatic chamber was carried out for another 15 hours with decreasing variations in relative humidity up to a limit value of 50%.

X-ray diffraction (XRD)

X-ray diffraction (XRD) of the geopolymeric precursors (kaolin and metakaolin) and of the geopolymers obtained from this precursor were performed using a D8 Advance Bruker diffractometer: diffractograms were obtained with a step of 0.02° and a step time of 2s. For the identification of the phases of the precursors (kaolin and metakaolin) and of the metakaolin geopolymers, this XRD method was used in the range $2\theta=5°\div70°$; the samples used for XRD analysis was prepared in powder form.

Fourier Transformed Infrared Spectroscopy (FTIR)

Fourier Transform Infrared (FTIR) spectroscopy is a powerful technique, which allows to characterize the vibrational and rotational motions of condensed matter systems excited by IR radiation [17-27]. IR spectroscopy covers the range of 14000-10 cm^{-1} of the electromagnetic spectrum; such a region can be divided into three different ranges: i) Near-IR (NIR) approximately 14000-4000 cm^{-1}; ii) Mid-IR (MIR) 4000-400 cm^{-1}, and iii) Far-IR 400-10 cm^{-1}. FTIR technique is, under some regards, complementary to Raman scattering, inelastic neutron scattering and density function simulations, these techniques furnishing valuable information on the rotational and vibrational motions as well as on the systems structural properties. Fourier Transform Infrared Spectroscopy (FTIR) can be used to evaluate the functional groups present both in the silico-aluminate precursors and in the metakaolin based geopolymers: moreover, this technique allows to define the time for the formation of the geopolymeric structure and, it also allows to follow the behavior of this geopolymeric structure at different treatment times in order to evaluate the stability of the same prepared geopolymeric matrices. The FTIR study was carried out in the range 4000-400 cm^{-1} with a resolution of 4 cm^{-1} and each spectrum was obtained after 32 scans on samples of kaolin (K), metakaolin (MK) and on three geopolymers obtained by metakaolin (MK) named MKG1, MKG2 and MKG3.

Raman Spectroscopy

As far as Raman spectroscopy is concerned, Raman spectra of precursors (kaolin and metakaolin) an of metakaolin based geopolymers were obtained by the Spectrometer BRAVO (Bruker Optics); the fount was formed by two lasers operating at the wavelength of 785 nm and 1064 nm. Investigated spectral range was 300-3200 cm^{-1} at the temperature of 25°C; spot size value was 10-15 micron at a magnification value of 10x lens. Moreover, a data preprocessing has been done; in particular, the correction of baseline and the reduction of the instrumental noise has been applied.

Results and Discussion

Brief description of the prepared samples

The hardened geopolymer pastes MKG 1,2,3 show somewhat similar chromatic (colour), physical (density, hardness, porosity) and mechanical (resistance and abrasion) characteristics. The differences observed are, in our opinion, largely attributable to the mixing procedure and less to the curing ones. For purely qualitative purposes, the image of one of the three prepared samples is shown in the following Figure 4.

Figure 4: Image of a representative fragment of the hardened geopolymer paste.

XRD analysis

The geopolymers diffractogram has not distinctive characteristics: these materials are amorphous regardless of the raw materials used and the process conditions. Generally, the XRD spectrum of a geopolymer is characterized by a wide "amorphous hump" for values of the diffraction angle 2θ≈27-29°: however, some authors have described the presence of crystalline or semicrystalline phases, such as zeolitic phases in the presence of a very diluted alkaline solution. Figure 5 illustrates the diffractograms of the precursors (kaolin and metakaolin) and of the geopolymers obtained from the same metakaolin. The kaolin shows a cristalline structure with narrow peaks due to the presence of kaolinite and quartz: as regards metakaolin, this precursor shows a large diffraction amorphous hump at values of 2θ between 8° and 20° related to its amorphous structure. Furthermore, in the XRD spectrum of this metakaolin precursor, some peaks related to quartz (SiO_2) have been detected. The alkaline activation of the metakaolin has determined the displacement of the "amorphous hump" towards higher diffraction angles: this is the amorphous phase, which consists of sodium aluminosilicate gel (N-A-S-H), and, it is a fundamental phase for the development of the mechanical properties of geopolymers obtained from metakaolin. Then, from Figure 5, observing the XRD spectra of two metakaolin based geopolymers (MKG1 and MKG2), we can see an amorphous structure, typical of geopolymers. Furthermore, the peak of quartz can still be observed in the metakaolin geopolymers, even after the geopolymerization reaction: this confirms its insolubility in this process of geopolymerization [28, 29].

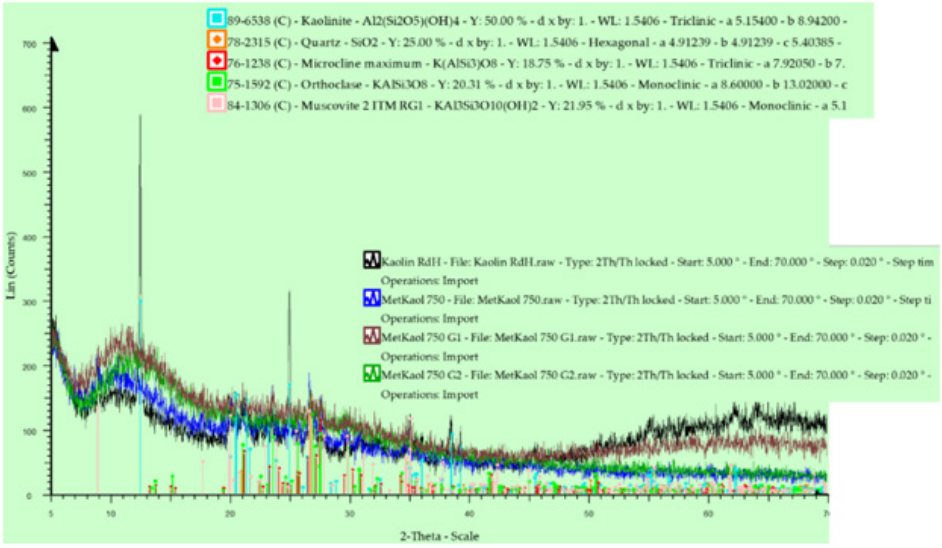

Figure 5: XRD spectra of kaolin, metakaolin and of metakaolin geopolymers (MKG1 and MKG2).

FTIR analysis

FTIR spectra of kaolin and metakaolin are given in Figure 6 the band positioned at 1114 cm^{-1} is attributed to Si–O stretching vibrations in kaolin structure (Figure 6). A significant band at 1001 cm^{-1} is assigned to Si–O–Si lattice vibration in kaolinite; sharp bands located at 950 and 910 cm-1 in the FTIR spectrum indicate surface OH bending and inner OH bending vibrations, that are mainly caused by Al–OH groups, respectively. Bands positioned at 750, 680 and 527 cm^{-1} in the low frequency region are related with Si–O and Al–O vibrations: specifically, the band centered at 527 cm^{-1} corresponds to Al(O,OH)6 octahedra in kaolinite. Another lower frequency band at 459 cm^{-1} is attributed to bending or stretching of T–O–T (T: Si or Al) bridge of aluminosilicates. Thermal treatment of kaolin at 750°C for 3h results in transformation of crystalline kaolin into amorphous metakaolin with the loss of internal water and dehydroxylation as it is evident from Figure 6. In this context, the characteristic bands observed in the FTIR spectrum of kaolin disappeared and broad features positioned at around 1036, 784 and 416 cm^{-1} appeared (Figure 6). High frequency band at 1036 cm^{-1} is attributed to stretching of Si–O bonds in amorphous SiO_2: moreover, band positioned at 527 cm^{-1} in kaolin is replaced by a broad band at 784 cm^{-1}, which is related to the vibrations of the AlO4 tetrahedron in metakaolin. FTIR band located at 459 cm^{-1} in the FTIR spectrum of kaolin indicating T–O–T (T: Si or Al) aluminosilicate bridge is seen in the FTIR spectrum of metakaolin as well displaying a broader peak compared to kaolin [30].

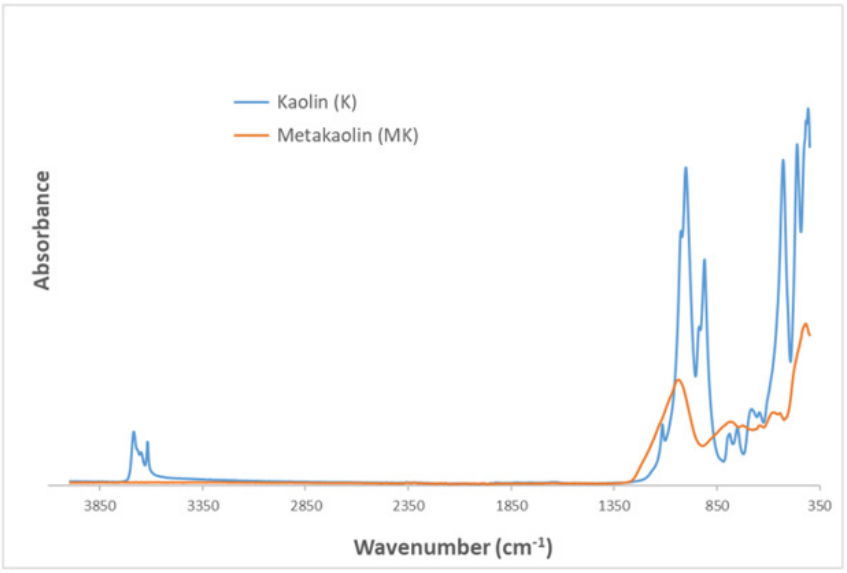

Figure 6: FTIR spectra kaolin and metakaolin.

Figure 7 shows the FTIR spectra of the three metakaolin-based geopolymers (MKG1, MKG2 and MKG3): they show similar vibration bands, typical of geopolymeric materials. In fact, the main IR bands observed for these geopolymers and their interpretation are shown in the following Table 2: it is noted that the most important vibration to consider when evaluating the formation of the geopolymeric structure is the Si-O-Si vibrational stretching at 1008–980 cm^{-1}.

Table 2: IR characteristic bands and their interpretation [31].

Absorption bands	Interpretation
3364 and 1652 cm^{-1}	Hydration water
1008–980 cm^{-1}	Si–O–Si stretching vibration
547 cm^{-1}	Si–O–Al bending vibration
450–470 cm^{-1}	Si–O–Si bending vibration
600–800 cm^{-1}	Al–O–Si vibrations
1460 cm^{-1}	Na_2CO_3

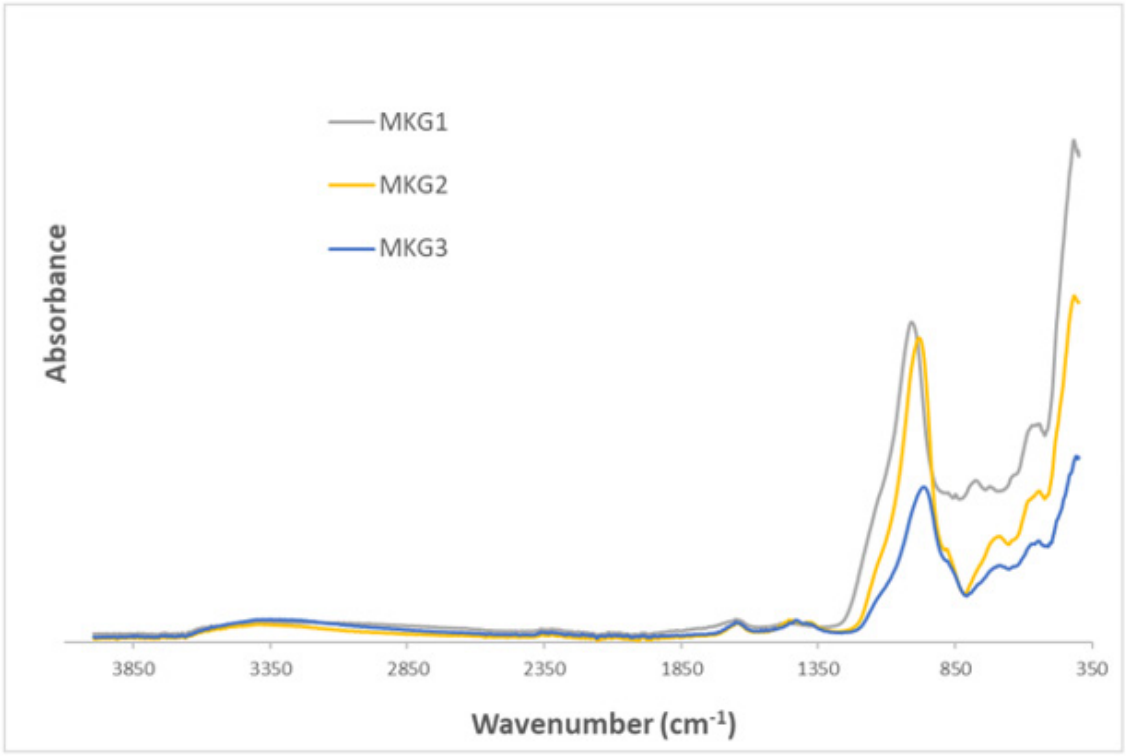

Figure 7: FTIR spectra of MKG1, MKG2 and MKG3.

Furthermore, according to some researchers [32,33], it is possible to define, regardless of the starting precursors used for the geopolymers preparation, that the formation of the geopolymeric structure occurs when we observe a shift of the main band related to Si–O–Si stretching vibration positioned at 1008-980 cm^{-1} in the FTIR spectrum of the geopolymer precursor of about 40 cm^{-1} with the consequent positioning of this band in the FTIR geopolymeric spectrum at 940 cm^{-1} (Figure 8).

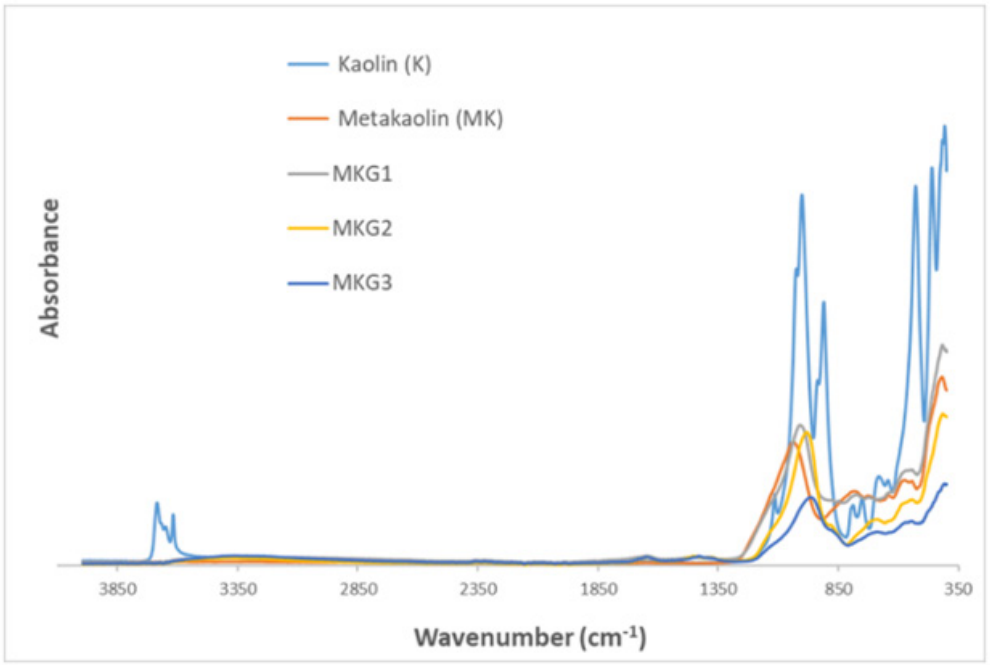

Figure 8: FTIR spectra of the precursors (kaolin and metakaolin) compared with the spectra of the geopolymeric samples (MKG1, MKG2 and MKG3).

Raman Spectroscopy analysis

In the Raman spectrum of pure kaolin (Figure 9), five distinct bands can be observed: the ν1–ν4 bands are assigned to the OH stretching mode of the three inner surface hydroxyl groups. Moreover, the band at 3620 cm^{-1} is assigned to the stretching mode of the inner hydroxyl group: the band at 3685 cm^{-1} is Raman active (infrared inactive), and it is observed as a component of an unresolved doublet at 3693–3685 cm^{-1}. The band at 3685 cm^{-1} is ascribed to the transverse optic mode, whereas the band at 3693 cm^{-1} is assigned to the longitudinal optic mode. This band is of low intensity in the Raman spectrum, but it is strongly infrared active. The 3670 and 3652 cm^{-1} bands (ν_2 and ν_3) are weak and, they are described as the out-of-phase vibrational modes of the in-phase vibration observed at 3693 cm^{-1}. The 3620 cm^{-1} OH band (ν5) is strong and sharp: the intensity of the OH stretching bands depends on the structural order of the kaolin [34].

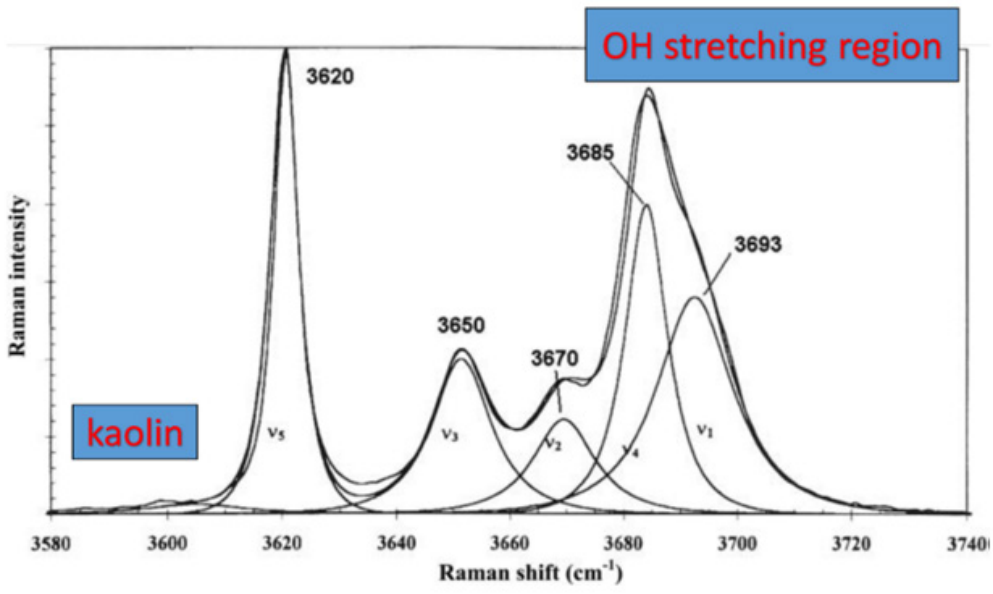

Figure 9: Raman spectra of the pure kaolin OH stretching region [34].

In addition to the OH stretching region, the most important spectral ranges observed in the Raman spectrum of kaolin (Figure 10) are those of the Si-O (1090 cm^{-1}), the OH bending (937 and 914 cm^{-1}), and the OH translational (795 and 755 cm^{-1}) vibrations.

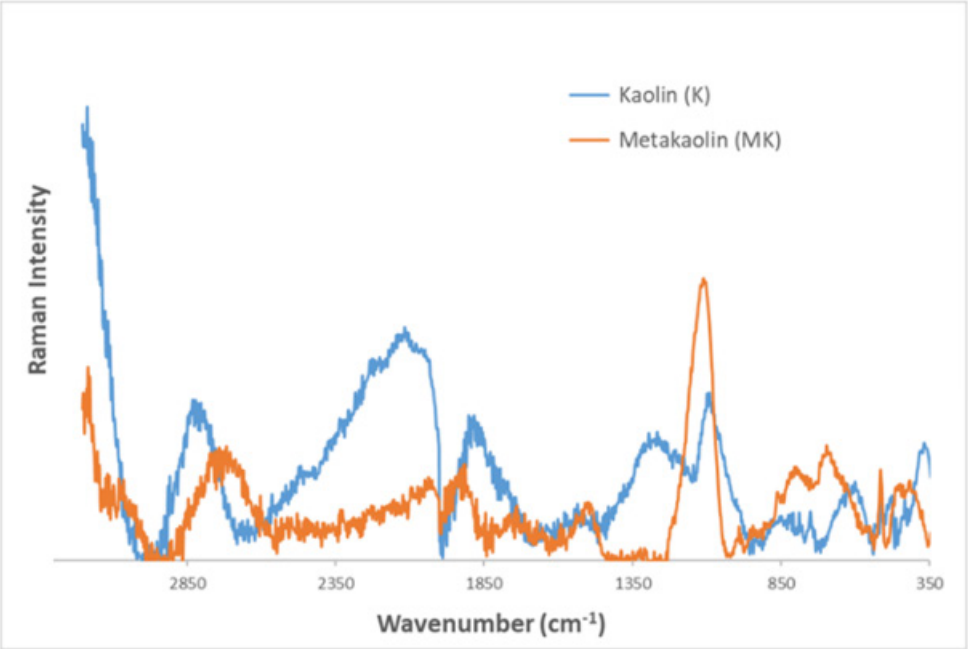

Figure 10: Raman spectra of kaolin and metakaolin.

The most important spectral bands observed in the Raman spectrum of pure metakaolin (Figure 10) are those of the Si-O stretching vibration (1110 cm^{-1}) and of silica (SiO_2) vibration (514 cm^{-1}) [35].

Table 3: Raman bands of geopolymers [36-37].

Absorption bands	Interpretation
590 cm^{-1}	Silica or silica glass
662 cm^{-1}	Si–O–Si

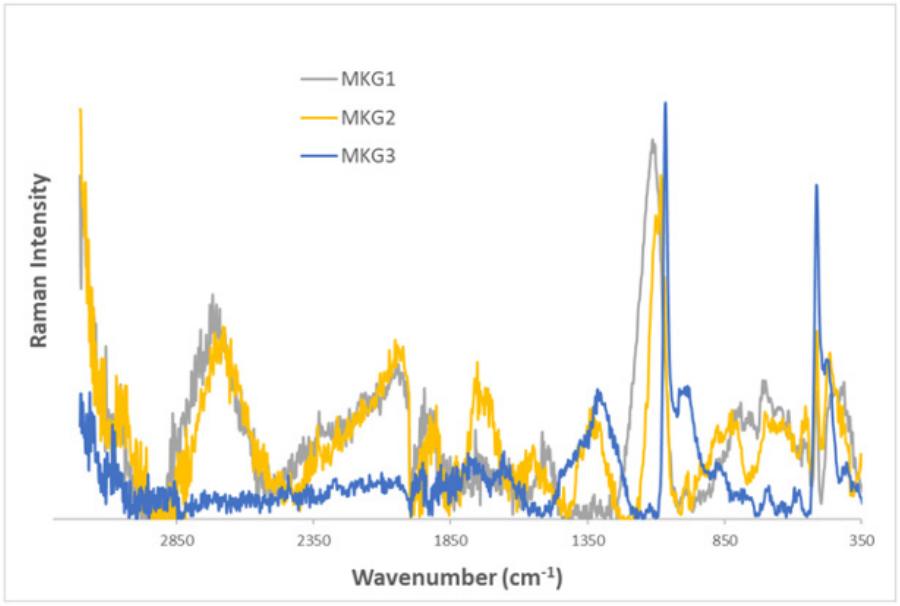

Figure 11: Raman spectra of MKG1, MKG2 and MKG3.

Furthermore, Raman spectroscopy was performed on the three metakaolin based geopolymers named MKG1, MKG2 and MKG3 (Figure 11): the Raman spectra of metakaolin geopolymers are characterized by the typical Raman bands of geopolymers (Table 3). The peak at 590 cm^{-1} can be assigned to a vibration of silica or silica glass and the band located at 662 cm^{-1} can be assigned can be assigned to Si–O–Si stretching [36,37].

Conclusion

In this article, geopolymeric pastes have been effectively prepared using metakaolin as a precursor and as an activating alkaline solution a mixture of an 8M solution of NaOH, in which sodium trisilicate powders have been dissolved: the geopolymerization process took place at T=80°C. The experimental characterization of precursors such as kaolin and metakaolin and of the metakaolin based geopolymers was carried out by X-ray diffractometry (XRD), Raman spectroscopy and Fourier transform infrared spectroscopy (FTIR). These techniques showed the complete calcination of the kaolin with the consequent conversion from crystalline kaolin to amorphous metakaolin, and, furthermore, the formation of the typical geopolymeric amorphous structure is observed.

Author Contributions: Conceptualization, visualization, methodology, M.T.C, G.M, L.M. and S.M.; formal analysis, M.T.C., G.M.; investigation, M.T.C, G.M and S.M.; writing-original draft preparation, M.T.C, G.M, L.M, S.M.; writing - review and editing, S.M and L.M.; supervision and project administration, S.M.; All authors have read and agreed to the published version of the manuscript.

Funding

We have not received any funding from the project for this publication.

Acknowledgment

In this section you can acknowledge any support given which is not covered by the author contribution or funding sections. This may include administrative and technical support, or donations in kind (e.g., materials used for experiments).

Conflicts of Interest

The authors declare no conflict of interest.

References

1. C Leonelli, M Romagnoli (2013) Geopolimeri: Polimeri inorganici attivati chimicamente. Seconda Edizione. ICerS.
2. Ch Panagiotopoulou, E Kontori, Th Perraki, G Kakali (2007) Dissolution of aluminosilicate minerals and by-products in alkaline media. Journal of Material Science 42: 2967-2973.
3. Sara Moutinho, Cristiana Costa, Slavka Andrejkovicˇová, Luís Mariz, Cristina Sequeira, et al. (2020) Assessment of properties of metakaolin-based geopolymers applied in the conservation of tile facades. Construction and Building Materials 259: 119759.
4. Tao Bai, Bowen Liu, Yanguang Wu, Wei Huang, Hao Wang, et al. (2020) Mechanical properties of metakaolin-based geopolymer with glass fiber reinforcement and vibration preparation. Journal of Non-Crystalline Solids 544: 120173.
5. J Davidovits (1991) Geopolymers - Inorganic polymeric new materials, J. Therm. Anal 37: 1633-1656.
6. J Davidovits (1994) Properties of geopolymer cements. First international conference on alkaline cements and concretes, Kiev, Ukraine, VIPOL Stock Company.
7. P Duxson, A Fernández-Jiménez, J L Provis, G C Lukey, A Palomo, et al. (2007) Geopolymer technology: the current state of the art. J Mater Sci 42: 2917-2933.
8. R Aiello, F Crea, A Nastro, B Subotic´, F Testa (1991) Influence of cations on the physicochemical and structural properties of aluminosilicate gel precursors. Part 1. Chemical and thermal properties. Zeolites 11(8): 767-775.
9. II Ivanova, R Aiello, JB Nagy, F Crea, EG Derouane, et al. (1994) Influence of cations on the physicochemical and structural properties of aluminosilicate gel precursors: II. Multinuclear magnetic resonance characterization. Micropor Mater 3(3): 245-257.
10. P Duxson, JL Provis, GC Lukey, SW Mallicoat, WM Kriven, et al. (2005) Understanding the relationship between geopolymer composition, microstructure and mechanical properties. Colloid. Surf A 269(1-3): 47-58.
11. P Rovnanik (2010) Effect of curing temperature on the development of hard structure of metakaolin-based geopolymer. Constr. Build. Mater 24(7): 1176-1183.
12. JW Phair, JD Smith, JSJ Van Deventer (2003) Characteristics of aluminosilicate hydrogels related to commercial “geopolymers”. Mater. Lett 57(28): 4356-4367.
13. Peng Zhang, Kexun Wang, Qingfu Li, Juan Wang, Yifeng Ling, et al. (2020) Fabrication and engineering properties of concretes based on geopolymers/alkali-activated binders - A review. Journal of Cleaner Production 258: 120896.
14. MF Zawrah, SE Abo Sawan, RM Khattab, Ayman A Abdel-Shafi (2020) Effect of nano sand on the properties of metakaolin-based geopolymer: Study on its low rate sintering. Construction and Building Materials 246: 118486.
15. Yanguang Wu, Bowen Lu, Tao Bai, Hao Wang, Feipeng Du, et al. (2019) Geopolymer, green alkali activated cementitious material: Synthesis, applications and challenges, Construction and Building Materials 224: 930-949.
16. E Papa (2010-2011) “Produzione e caratterizzazione di schiume inorganiche a base geopolimerica”, Tesi di laurea magistrale, Dipartimento di Chimica Industriale e dei Materiali, Università degli Studi di Bologna.
17. Migliardo F, Magazù S, Caccamo MT (2013) Infrared, Raman and INS Studies of Poly-Ethylene Oxide Oligomers. Journal of Molecular Structure 1048: 261-266.
18. Strangman G, Boas DA, Sutton JP (2002) Non-invasive neuroimaging using near-infrared light. Biol. Psych 52(7): 679-93.
19. Villringer A, Chance B (1997) Non-invasive optical spectroscopy and imaging of human brain function. Trends Neurosci 20(10): 435-42.
20. Doménech Carbó MT, Bosch Reig F, Gimeno Adelantado JV, Periz Martínez V (1996) Fourier transform infrared spectroscopy and the analytical study of works of art for purposes of diagnosis and conservation. Anal. Chim. Acta 330(2-3): 207-215.
21. Rohman A, Che Man YB (2009) Analysis of cod-liver oil adulteration using Fourier transform infrared (FTIR) spectroscopy. J. Am. Oil Chem. Soc 86: 1149-1153.
22. Coates J (2006) Interpretation of infrared spectra, a practical approach. Encycl. Anal. Chem 10815-10837.
23. Deepa M, Sharma N, Agnihotory SA, Chandra R (2001) FTIR investigation on ion-ion interaction in liquid and gel polymeric electrolytes-LiCF3SO3-PC-PMMA. J. Mater. Sci 37: 1759-1765.

24. Suthanthiraraj SA, Kumar RJ, Paul B (2009) Vibrational spectroscopic and electrochemical characteristics of Poly (Propylene Glycol)-silver triflate polymerelectrolyte system. Ionics 16: 145-151.

25. Winie T, Arof AK (2006) FT-IR studies on interactions among components in hexanoyl chitosan-based polymer electrolytes. Spectrochim. Acta A 63(3): 677-684.

26. Duval M, Gross E (2013) Degradation of poly (ethylene oxide) in aqueous solutions by ultrasonic waves. Macromolecules 46: 4972-4977.

27. Magazù S (2000) NMR, static and dynamic light and neutron scattering investigations on polymeric aqueous solutions. J. Mol. Struct 523(1-3): 47-59.

28. Nur Ain Jaya, Liew Yun-Ming, Heah Cheng-Yong, Mohd Mustafa Al Bakri Abdullah, Kamarudin Hussin, et al. (2020) Correlation between pore structure, compressive strength and thermal conductivity of porous metakaolin geopolymer. Construction and Building Materials 247: 118641.

29. Anil Kumar Thakur, Asokan Pappu, Vijay Kumar Thakur (2019) Synthesis and characterization of new class of geopolymer hybrid composite materials from industrial wastes. Journal of Cleaner Production 230: 11-20.

30. Isil Ozer, Sezen Soyer-Uzun (2015) Relations between the structural characteristics and compressive strength in metakaolin based geopolymers with different molar Si/Al ratios. Ceramics International 41(8): 10192-10198.

31. Isabella Lancellotti, Michelina Catauro, Chiara Ponzoni, Flavia Bollino, Cristina Leonelli, et al. (2013) Inorganic polymers from alkali activation of metakaolin: Effect of setting and curing on structure. Journal of Solid State Chemistry 200: 341-348.

32. E Prud'homme, A Autef, N Essaidi, P Michaud, B Samet, et al. (2013) Defining existence domains in geopolymers through their physicochemical properties. Appl. Clay Sci 73: 26-34.

33. Isabella Lancellotti, Maria Cannio, Flavia Bollino, Michelina Catauro, Luisa Barbieri, et al. (2015) Geopolymers: An option for the valorization of incinerator bottom ash derived "end of waste", Ceramics International 41(2A): 2116-2123.

34. Erzsébet Horváth, János Kristóf, Ray L Frost (2010) Vibrational Spectroscopy of Intercalated Kaolinites. Part I. Applied Spectroscopy Reviews 45(2): 130-147.

35. Jamil R Memon, Keith R Hallam, Muhammad I Bhanger, Adel El-Turki, Geoffrey C Allen, et al. (2009) Evaluation of sorption of uranium onto metakaolin using X-ray photoelectron and Raman spectroscopies. Analytica Chimica Acta 631(1): 69-73.

36. McMillan P (1984) Structural studies of silicate glasses and melts-applications and limitations of Raman spectroscopy. Am Mineral 69: 622-644.

37. Dai W, Zhu M, Hou YD, Wang H, Yan H, et al. (2004) Preparation and characterization of $Ba_2TiSi_2O_8$ ferroelectric films produced by sol–gel method. Mater Lett 58(28-23): 2927-2931.